Available online at www.sciencedirect.com
ScienceDirect
Bioorganic & Medicinal Chemistry Letters
Bioorganic & Medicinal Chemistry Letters 17 (2007) 3550–3557

Novel inhibitors of VEGF receptors-1 and -2 based on azole-5-carboxamide templates

Alexander S. Kiselyov,[a,*] Daniel Milligan[b] and Xiaohu Ouyang[b]

[a]*Small Molecule Drug Discovery, Chemical Diversity, Inc., 11558 Sorrento Valley Road, San Diego, CA 92121, USA*
[b]*Department of Chemistry, ImClone Systems, Inc., 180 Varick Street, New York, NY 10014, USA*

Received 29 March 2007; revised 17 April 2007; accepted 18 April 2007
Available online 22 April 2007

Abstract—We have developed a series of novel potent 1-(2-(pyridin-4-yl)ethyl)-1*H*-azole-5-carboxamides active against kinases VEGFR-2 and -1. Both specific and dual ATP-competitive inhibitors of VEGFR-2 were identified. Kinase selectivity could be controlled by varying the 5-carboxamide substituent at the azole ring. The most specific molecules displayed >10-fold selectivity for VEGFR-2 over VEGFR-1. Compound activities in vitro and in cell-based assays (IC_{50} < 100 nM) were similar to those of reported clinical and development candidates, including PTK787 (Vatalanib[trade]) and ZD6474 (Vandetanib™). High permeability of active compounds across the Caco-2 cell monolayer (>40×10^{-5} cm/min) is indicative of their potential for intestinal absorption upon oral administration.

Angiogenesis or formation of new blood vessels, is involved in embryonic development,[1,2] follicular growth, and wound healing as well as in pathological conditions such as tumor growth and degenerative eye conditions.[3–6] Cancer cells easily acquire resistance toward conventional cytotoxic agents commonly used for chemotherapy. It is believed that this issue could be addressed by anti-angiogenesis therapy targeting tumor vascular endothelial cells.[1] Vascular endothelial growth factors (VEGFs) have been implicated in regulation of angiogenesis in vivo.[7,8] VEGFs mediate their biological effect through high affinity VEGF receptors which are expressed on the endothelial cells.[9] These include receptor tyrosine kinases, VEGFR-1 (Flt-1) and VEGFR-2 (Kinase insert domain receptor (KDR) or flk1).[10,11] In early embryogenesis, VEGFR-1 functions as a negative regulator, most likely through its strong VEGF-A trapping activity. In adults, VEGFR-1-specific ligands are reported to induce mild angiogenesis. VEGFR-2 is the major positive signal transducer for endothelial cell proliferation and differentiation at all mammalian stages of development.[12] Overexpression of both VEGF and VEGFR was reported for most of the clinically important human solid cancers. Consequently, modulation of VEGF/VEGFR signaling activity offers an attractive target for inhibition of an aberrant angiogenesis and suppression of tumor growth.[12]

Several groups in the industry have developed methods for sequestering VEGF which leads to a signal blockade via VEGF receptors and, subsequently to an inhibition of a malignant angiogenesis. Perhaps, the most successful marketed agent reportedly working via this mechanism is Avastin™.[13,14] A number of small-molecule inhibitors affect VEGF/VEGFR signaling by directly competing with the ATP-binding site of the respective intracellular kinase domain. This event leads to the blockade of a VEGFR phosphorylation and, ultimately to the apoptotic death of the aberrant endothelial cells. Phase III and II clinical candidates PTK787 (Vatalanib™, **1**) and ZD6474 (Vandetanib™, **2**) that exhibit this mechanism of action were shown to be active against various cancers (Fig. 1).[15–17] The pyridazine ring of the phthalazine template in PTK787 **1** and its analogue BAY579352 (**6**) has been replaced with the isosteric anthranyl amide derivatives **3**, **4**, and AMG-706 (**5**).[12] Intramolecular hydrogen bonding was suggested to be responsible for the optimal spatial orientation of the pharmacophore pieces, similar to that of the parent PTK787.[18]

The essential pharmacophore elements for the VEGFR-2 activity of phthalazine-based molecules and their ana-

Keywords: Vascular endothelial growth factor receptor-2; VEGFR-2; VEGFR-1; Receptor tyrosine kinase; Dual kinase inhibitors; Angiogenesis; 1-(2-(Pyridin-4-yl)ethyl)-1*H*-azole-5-carboxamides.
* Corresponding author. Tel.: +1 858 794 4860; fax: +1 858 794 4190; e-mail: ask@chemdiv.com

0960-894X/$ - see front matter © 2007 Elsevier Ltd. All rights reserved.
doi:10.1016/j.bmcl.2007.04.042

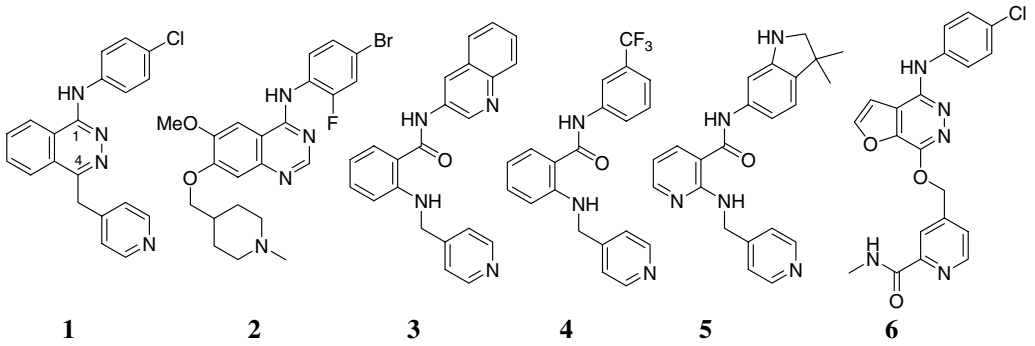

Figure 1. Selected inhibitors of VEGFR-2.

logues (**1**, **3**–**6**) include (i) [6,6] fused (or related) aromatic system; (ii) *para*- or 3,4-di-substituted aniline function in position 1 of the phthalazine core; (iii) hydrogen bond acceptor (Lewis base: lone pair(s) of a nitrogen or oxygen atom(s)) attached to position 4 via an appropriate linker (aryl or fused aryl group).In this communication, we expand upon our initial findings[19,20] and disclose potent inhibitors of VEGFR-2 kinase based on 1-(2-(pyridin-4-yl)ethyl)-1*H*-azole-5-carboxamide template. We reasoned that this scaffold could provide for the proper pharmacophore arrangement relevant to molecules **1**, **3**–**6**.[21–23] In addition, we focused on finding optimized pharmacophores to yield most potent specific and dual VEGFR-2 compounds with potential for oral availability. An effect of carboxamide substitution (H for alkyl) on the overall activity has been evaluated as well.

Targeted azole-5-carboxylates (Table 1, **9**–**53**) were prepared by a concise synthetic sequence from the respective NH-heterocycles **7** via (a) Michael addition of azolyl anions generated from **7** (NaH/DMF, RT, 8 h) to vinyl pyridines (Ar^2 = 2-, 3- or 4-pyridyl) (*path A*, Scheme 1)[24a] or (b) base-promoted (NaH/DMF, RT, 4 h) nucleophilic displacement of the terminal tosyl group in azolylpropyl tosylates (*path B*, Scheme 1)[24b,4c] to afford the desired 1-(2-(aryl-4-yl)ethyl)-1*H*-azole esters **8a** or **8b**. These where hydrolyzed with a 10% aq LiOH at RT for 2 h to yield free acids. The acids were subsequently coupled to the set of aromatic amines Ar^1NH_2 using EDCI/HOAt/Hunig's base in CH_2Cl_2 at RT to furnish the targeted azoles in 35–57% overall yields.[25]

Compounds (**9**–**53**, Table 1) were tested in vitro against isolated VEGFR-2 kinase. Specifically, we measured their ability to inhibit phosphorylation of a biotinylated polypeptide substrate (p-GAT, CIS Bio International) in a homogeneous time-resolved fluorescence (HTRF) assay at an ATP concentration of 2 μM. The results were reported as a 50% inhibition concentration value (IC_{50}). Literature VEGFR-2 inhibitors **1**–**4** (Table 1) were included as internal standards for quality control.[26]

As seen from Table 1, a number of azoles exhibited a sound inhibitory activity against VEGFR-2. By varying i) carboxamide (Ar^1); (ii) 1-(2-(aryl-4-yl)ethyl (Ar^2) substituents, and (iii) heterocyclic core, we modulated compounds' potency against the enzyme. Initial experiments in the pyrazole series (entries **9**–**17**, Table 1) suggested that 2-(pyrid-4-yl)ethyl group yields the best activity with the IC_{50} value of 77 nM against VEGFR-2 (compound **11**). Molecules featuring 2-(pyrid-2-yl)ethyl (**9**) and 2-(pyrid-3-yl)ethyl (**10**) groups showed no activity in the VEGFR-2 assay (IC_{50} > 10 μM). Furthermore, substitution of pyrazole with a number of alternative functionalities isoelectronic to 1-(2-(aryl-4-yl)ethyl group failed to yield enzyme inhibitors (Table 1, entries **12**–**17**). This fact could be explained by the proper alignment of the lower portion of the molecule, namely nitrogen atoms (Lewis base, hydrogen bond acceptors) of 4-pyridyl-group with the *Arg*1302 moiety in the ATP-binding pocket of VEGFR-2. We further reasoned that in **9** and **10** the nitrogen of the pyridine ring and lone pairs of methylenedioxy group in derivatives **12** and**14** are likely to be mis-aligned with the *Arg*1302.[28,29] Similarly, 4-isoxazolo- (**15**), 3-benzoxazolo- (**16**), and 4-imidazolo- (**17**) pharmacophoresare not properly accommodated in the binding pocket.[19–23] Following these data, we decided to continue optimization of pyrazole derivatives featuring 2-(pyrid-4-yl)ethyl group.

In studying SAR of the ***5-carboxamide*** portion of the molecule, we varied the aniline substituent (Ar_1) (Table 1, entries **18**–**34**). Gratifyingly, several *para*-substituted anilines allowed for the improved potency of the final pyrazoles in VEGFR-2 assays. For example, hydrophobic alkyl or CF_3 moieties yielded compounds with 28–74 nM potencies in the enzymatic assay. The molecules substituted with *p*-Et, *p*-*i*-Pr-, and *p*-*t*-Bu-groups displayed increased potencies 120 nM (**19**), 74 nM (**24**), and 42 nM (**23**), respectively, suggesting presence of a hydrophobic pocket in the binding site of VEGFR-2. The 4-ClF_2CO-group (**22**) resulted in the best activity in this series (IC_{50} = 17 nM). Both 4-F_3C- and 4-F_3CO-derivatives (**18**, **20**) also inhibited VEGFR-2 (IC_{50}'s of 69 and 28 nM, respectively). Similar *meta*-substitution led to considerably less potent molecule (Ar_1 = 3-F_3CO- (**21**), IC_{50} = 370 nM). Larger functionalities in the *para*-position of the Ar_1 were not tolerated. For example, gradual increase in size of the 4-substituent in molecules **25**, **26**, and **27** (from *para*-Ph to *para*-OCH_2Ph) resulted in completely inactive molecules. We speculated that these functions cannot be properly accommodated in the hydrophobic pocket of VEGFR-2.[28,29] As compared to the molecule **C**, 3-(quinolyl)

Table 1. Activity of azoles **9**–**53** against VEGFR-1 and VEGFR-2

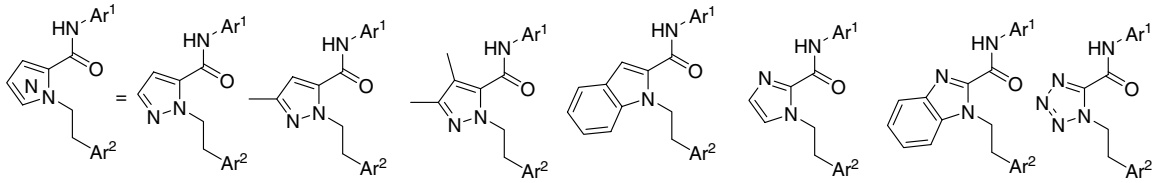

Azoles **(9-53)** ***Pyraz*** **(9-34)** ***3-Me-Pyraz*** **(35,36)** ***3,4-diMe-Pyraz*** **(37,38)** ***Indole*** **(39,40)** ***Im*** **(41-45)** ***Bz*** **(46-48)** ***Tetraz*** **(49-53)**

Compound	Azole	Ar^1	Ar^2	VEGFR-2, enzymatic, IC_{50}[a] (μM)	VEGFR-1, enzymatic, IC_{50}[a] (μM)	VEGFR-2, cell-based ELISA, IC_{50}[a] (μM)
1, **PTK787**				0.054 ± 0.006 (0.042 ± 0.003)[b]	0.14 ± 0.02 (0.11 ± 0.03)[b]	0.021 ± 0.03 (0.016 ± 0.001)[c]
2, **ZD6474**				0.022 ± 0.003 (0.017 ± 0.003)[b]	0.10 ± 0.01 (0.09 ± 0.01)[b]	1.66 ± 0.11 (2.70 ± 0.17)[c]
3				0.032 ± 0.005 (0.023 ± 0.006)[b]	0.17 ± 0.05 (0.130 ± 0.081)[b]	0.09 ± 0.01 (0.0012 ± 0.0002)[c]
4				0.015 ± 0.004 (0.009 ± 0.001)[b]	0.16 ± 0.05 (0.13 ± 0.03)[b]	0.05 ± 0.01 (0.0012 ± 0.0001)[c]
9	***Pyraz***	4-Cl(C_6H_4)	2-Pyridine	>10	>10	>10
10	***Pyraz***	4-Cl(C_6H_4)	3-Pyridine	>10	>10	>10
11	***Pyraz***	**4-Cl(C_6H_4)**	**4-Pyridine**	**0.077 ± 0.005**	**0.097 ± 0.01**	**0.09 ± 0.01**[d]
12	***Pyraz***	4-Cl(C_6H_4)	5-Piperonyl	>10	>10	>10
13	***Pyraz***	4-Cl(C_6H_4)	3,4-Di-F(C_6H_4)	>10	>10	>10
14	***Pyraz***	4-Cl(C_6H_4)	3,4-Di-MeO(C_6H_4)	>10	>10	>10
15	***Pyraz***	4-Cl(C_6H_4)	4-Isoxazolo	>10	>10	>10
16	***Pyraz***	4-Cl(C_6H_4)	3-Benzisoxazolo	>10	>10	>10
17	***Pyraz***	4-Cl(C_6H_4)	4-Imidazolo	>10	>10	>10
18	***Pyraz***	**4-F_3C(C_6H_4)**	**4-Pyridine**	**0.069 ± 0.007**	**0.38 ± 0.02**	**0.048 ± 0.004**
19	***Pyraz***	**4-Et(C_6H_4)**	**4-Pyridine**	**0.12 ± 0.008**	**0.22 ± 0.01**	**0.086 ± 0.007**
20	***Pyraz***	**4-F_3CO(C_6H_4)**	**4-Pyridine**	**0.028 ± 0.002**	**0.19 ± 0.01**	**0.018 ± 0.002**
21	***Pyraz***	3-F_3CO(C_6H_4)	4-Pyridine	0.37 ± 0.04	0.45 ± 0.05	0.28 ± 0.04
22	***Pyraz***	**4-ClF_2CO(C_6H_4)**	**4-Pyridine**	**0.017 ± 0.003**	**0.32 ± 0.04**	**0.021 ± 0.003**
23	***Pyraz***	**4-*t*-Bu(C_6H_4)**	**4-Pyridine**	**0.042 ± 0.005**	**0.59 ± 0.04**	**0.033 ± 0.002**
24	***Pyraz***	**4-*i*-Pr(C_6H_4)**	**4-Pyridine**	**0.074 ± 0.004**	**0.44 ± 0.06**	**0.053 ± 0.005**
25	***Pyraz***	4-Ph(C_6H_4)	4-Pyridine	0.95 ± 0.07	2.25 ± 0.11	1.56 ± 0.18
26	***Pyraz***	4-PhO(C_6H_4)	4-Pyridine	3.22 ± 0.28	5.25 ± 0.54	>10
27	***Pyraz***	4-$PhCH_2O$(C_6H_4)	4-Pyridine	>10	>10	>10
28	***Pyraz***	3-(Quinolinyl)	4-Pyridine	0.18 ± 0.01	0.38 ± 0.05	1.22 ± 0.08
29	***Pyraz***	5-(Indazolyl)	4-Pyridine	5.15 ± 0.22	>10	>10
30	***Pyraz***	6-(Indazolyl)	4-Pyridine	>10	>10	>10
31	***Pyraz***	3-CF_3,4-Cl(C_6H_4)	4-Pyridine	0.75 ± 0.06	2.33 ± 0.25	0.45 ± 0.06
32	***Pyraz***	**3-Cl,4-CF_3(C_6H_4)**	**4-Pyridine**	**0.18 ± 0.03**	**0.98 ± 0.12**	**0.095 ± 0.01**
33	***Pyraz***	3,4-Di-Cl(C_6H_4)	4-Pyridine	0.26 ± 0.05	0.86 ± 0.11	0.12 ± 0.02
34	***Pyraz***	3,4-Di-MeO(C_6H_4)	4-Pyridine	0.44 ± 0.12	1.23 ± 0.22	0.075 ± 0.006[e]
35	***3-Me-Pyraz***	4-Cl(C_6H_4)	4-Pyridine	0.78 ± 0.03	1.22 ± 0.06	2.54 ± 0.33
36	***3-Me-Pyraz***	4-F_3CO(C_6H_4)	4-Pyridine	1.19 ± 0.08	2.25 ± 0.12	1.34 ± 0.22
37	***3,4 diMe-Pyraz***	4-Cl(C_6H_4)	4-Pyridine	> 10	>10	>10

38	***3,4 diMe-Pyraz***	4-$F_3CO(C_6H_4)$	4-Pyridine	>10	>10	>10
39	***Indole***	4-$Cl(C_6H_4)$	4-Pyridine	>10	>10	>10
40	***Indole***	4-$F_3CO(C_6H_4)$	4-Pyridine	>10	>10	>10
41	***Im***	4-$Cl(C_6H_4)$	4-Pyridine	0.38 ± 0.04	0.94 ± 0.12	1.32 ± 0.19
42	***Im***	4-$F_3C(C_6H_4)$	4-Pyridine	0.47 ± 0.04	0.79 ± 0.10	1.66 ± 0.26
43	***Im***	4-$F_3CO(C_6H_4)$	4-Pyridine	0.79 ± 0.04	4.27 ± 0.28	1.05 ± 0.13
44	***Im***	4-*t*-$Bu(C_6H_4)$	4-Pyridine	0.94 ± 0.13	3.86 ± 0.11	2.25 ± 0.31
45	***Im***	3-Cl,4-$CF_3(C_6H_4)$	4-Pyridine	1.31 ± 0.22	4.56 ± 0.35	4.95 ± 0.56
46	***Bz***	4-$Cl(C_6H_4)$	4-Pyridine	>10	>10	>10
47	***Bz***	4-$F_3CO(C_6H_4)$	4-Pyridine	>10	>10	>10
48	***Bz***	3-Cl,4-$CF_3(C_6H_4)$	4-Pyridine	>10	>10	>10
49	***Tetraz***	4-$Cl(C_6H_4)$	4-Pyridine	0.64 ± 0.07	0.89 ± 0.15	2.03 ± 0.22
50	***Tetraz***	4-$F_3C(C_6H_4)$	4-Pyridine	0.85 ± 0.11	1.08 ± 0.13	2.96 ± 0.34
51	***Tetraz***	4-$F_3CO(C_6H_4)$	4-Pyridine	2.65 ± 0.36	3.88 ± 0.37	2.97 ± 0.42
52	***Tetraz***	4-*t*-$Bu(C_6H_4)$	4-Pyridine	>10	>10	>10
53	***Tetraz***	3-Cl,4-$CF_3(C_6H_4)$	4-Pyridine	>10	>10	>10

[a] IC_{50} values were determined from the logarithmic concentration-inhibition point (ten points). The important values are given as means of at least two duplicate experiments.
[b] Literature IC_{50} values,[18] as measured at 8 μM ATP.
[c] Literature data[18] correspond to the inhibition of VEGF-induced phosphorylation of VEGFR-2 in CHO cells.
[d] Molecules with best enzymatic and cellular potencies against VEGFR-2 are ***bolded***.
[e] Molecule **34** was found to be cytotoxic for 293 cells (GI_{50} concentration is given).[27]

group in our pyrazole series (**28**) afforded less potent molecule (IC_{50} = 180 nM). Similar 5- and 6-(indazolyl) substitution yielded inactive molecules (Table 1, **29**, **30**). 3,4-Di-substituted aniline entries also yielded potent compounds. Examples include 3-Cl-4-CF_3- (**32**; IC_{50} = 180 nM), 3,4-di-Cl- (**33**; IC_{50} = 260 nM), and 3,4-di-MeO (**34**, IC_{50} = 440 nM). However, the latter molecule was found to be cytotoxic in our cellular assay (Table 1).

In the next series of experiments, we evaluated both steric and electronic requirements for the heterocyclic template. Specifically, we have selected optimized set of substituents and varied the central core of the azole (Table 1). Alkyl substituents in positions 3 and 4 of the pyrazole template were not tolerated (entries **35**–**38**). For example, 3-methylpyrazole derivative **35** showed only marginal activity in the VEGFR-2 assay (IC_{50} = 780 nM, compare with **11**), whereas 3,4-dimethyl analogue **37** was completely inactive. Bulkier indole and benzimidazole templates (Table 1, entries **39**, **40**, and **46**–**48**, respectively) yielded inactive compounds. Interestingly, isoelectronic azoles, namely similar imidazole and tetrazole derivatives, consistently yielded less potent molecules, even when endowed with optimized substituents. For example, imidazole and tetrazole derivatives **41** and **49** featured activities of 340, and 680 nM, respectively, in VEGFR-2 enzymatic assay, whereas similar pyrrole compound showed an IC50 of 77 nM. Similar trend continued through other azole derivatives (Table 1, compare **18** (***Pyraz***), **42** (***Im***), and **50** (***Tetraz***); **20** (***Pyraz***), **43** (***Im***), and **51** (***Tetraz***)). Pyrazole derivatives displayed 10- to 50-fold better potency against VEGFR-2. We reasoned that there is relatively tight pocket to accommodate azole template. It is lined up with surrounded by *Leu*840, *Val*848, *Val*899, *Phe*918, and *Leu*1035 moieties (Fig. 2).[28,29] Notably, unsubstituted amide N**H**CO function of the 5-carboxamide substituent is critical for the activity against both VEGFR-2 and VEGFR-1. Displacement of H with Me group in the amide function of **11** (compound **54**) led to the completely inactive molecule against both kinases (IC_{50} > 10 μM), despite the optimized Ar_1 (4-$Cl(C_6H_4)$) and Ar_2 (4-pyridyl) substituents.

Five selected VEGFR-2 inhibitors, namely **11**, **20**, **22**, **23**, and **32**, tested ATP-competitive in the radioassay. Competition assays were conducted with varying concentration (0–100 μM) of ATP. Specifically, 5 different concentrations of ^{32}P ATP were incubated with VEGFR-2 in the absence, IC_{50} or IC_{90} concentration of the inhibitors for 45 min at RT. A double reciprocal graph of the degree of phosphorylation (1/cpm) against ATP-concentration (1/[ATP]) was plotted.The data were analyzed by a non-linear least-squares program to determine kinetic parameters using GraphPad software. Determined K_i values for the three selected compounds are listed in Table 2.

Compounds **9**–**53** were also tested via HTRF format against VEGFR-1. The results in Table 1 indicate that many VEGFR-2 active azole-5-carboxamides display good activity against VEGFR-1 as well. For the most potent compounds, the IC_{50} values were in 97–590 nM

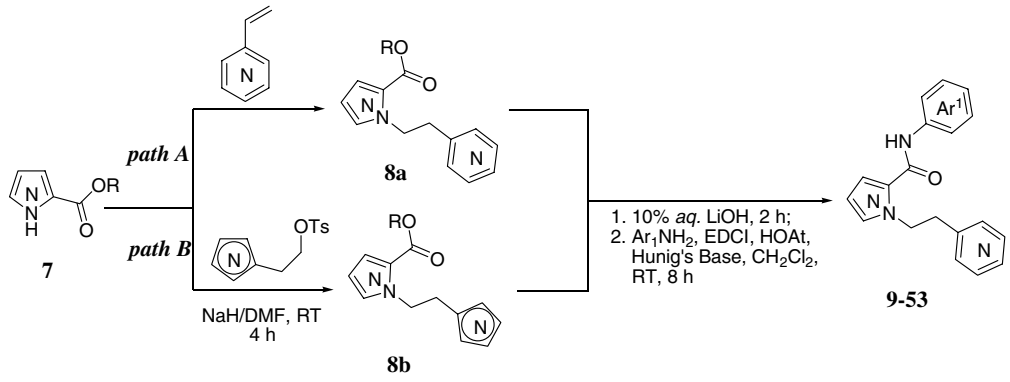

Scheme 1.

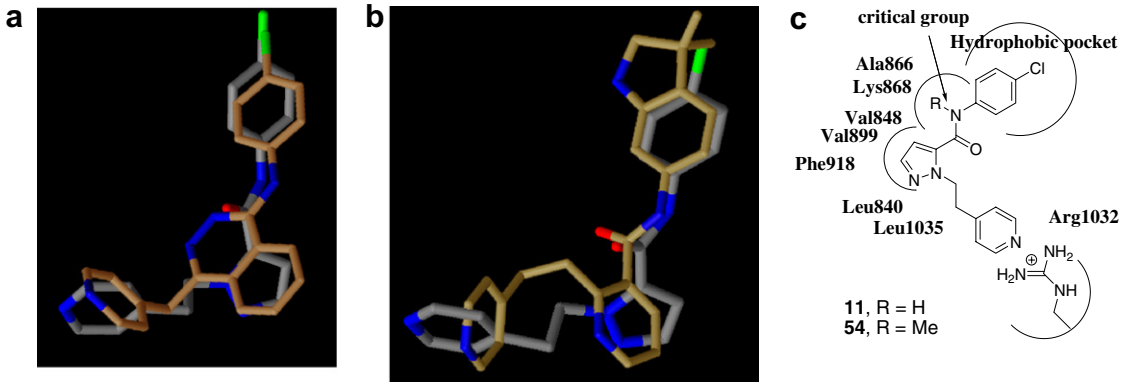

Figure 2. Structural overlap between (a) **11** (gray) and Vatalanib™ (**1**, brown); (b) **11** (gray) and AMG-706 (**4**, brown); (c) pharmacophore hypothesis for the mode of binding of azole-5-carboxylates within the ATP binding pocket of VEGFR-2. Central phenyl ring is surrounded by *Leu*840, *Val*848, *Val*899, *Phe*918, and *Leu*1035. The triazole ring is in close proximity with the *Ala*866 and *Lys*868, and pyridine nitrogen is near *Arg*1032.

Table 2. Compounds **11**, **20**, **22**, **23**, and **32** are ATP-competitive inhibitors of VEGFR-2

Compound	K_i at IC_{50} (μM)	K_i at IC_{90} (μM)
11	0.11	0.09
20	0.09	0.08
22	0.07	0.09
23	0.13	0.14
32	0.17	0.16

range. This outcome could be of benefit in the clinical setting as both receptors are reported to mediate VEGF signaling in the angiogenesis.[12,30] Several compounds containing bulky *para*-substituted Ar^1 functions (Table 1, see **22**, **23**) yielded over 10-fold selectivity for the VEGFR-2 vs VEGFR-1 kinase. This observation suggests that it is possible to develop VEGFR-2 specific inhibitors lacking VEGFR-1 activity. Structural reasons for this VEGFR-2 specificity over VEGFR-1 are under further investigation. Screening of **9**–**53** against a number of other receptor (IGF1R, InR, FGFR1, Flt3, Flt4, ErbB1, ErbB2/Her2, c-Met) and cytosolic (PKA, GSK3β, PKB/Akt, bcr-Abl, Cdk1, Raf1, Cdk2) kinases revealed no significant crossreactivity (PI > 30%, triplicate measurements) at a screening concentration of 10 μM.

Active in vitro inhibitors of VEGFR-2 were further characterized in a cell-based phosphorylation ELISA (Table 1).[31] In general, good in vitro-to-cell based activity correlation has been found for these compounds. In our hands, the best molecules displayed 18–95 nM activity in inhibiting cell-based phosphorylation of VEGFR-2 comparable to late stage development candidates Vatalanib™ and Vandetanib™.[12] This fact indicates that a number of the title molecules, including **11**, **18**–**20**, **22**–**24**, **32**, could be further developed for in vivo studies as both VEGFR-2-specific and VEGFR-1/2-dual inhib-

Table 3. Passive diffusion potential across Caco-2 cell monolayer for selected compounds

Compound	Intrinsic permeability, P_m value × 10^{-5} cm/min	Absorption potential	Compound	Intrinsic permeability, P_m value × 10^{-5} cm/min	Absorption potential
C	38.6 (lit. 45.2)[6]	High	**20**	42.2	High
D	17.3 (lit. 21.7)[6]	Med	**22**	28.4	Med/high
11	41.7	High	**23**	44.6	High
18	38.5	High	**24**	49.1	High
19	58.2	High	**32**	27.6	Med/high

itors. Notably, although the molecule **34** (Table 1) displayed only moderate VEGFR-2 inhibition activity (IC_{50} = 440 nM), it showed good cellular activity (IC_{50} = 75 nM). However, additional cell-based experiments suggested that the molecule had a non-specific cytotoxicity.[27] High permeability of VEGFR-2 active compounds across Caco-2 cell monolayer ($>30 \times 10^{-5}$ cm/min) was indicative of their potential for intestinal absorption upon oral administration. Good correlation between cell-based activity and P_m values was observed for all active compounds (Table 3).

In summary, we have developed a series of novel potent azole-5-carboxamide derivatives active against kinases VEGFR-2 and -1. Both specific and dual ATP-competitive inhibitors of VEGFR-2 were identified. Kinase selectivity could be controlled by varying the carboxamide substituent at the azole ring. Several most specific molecules displayed >10-fold selectivity for VEGFR-2 over VEGFR-1. Compound activities in both in vitro and cell-based assays (IC_{50} < 100 nM) were similar to those of the reported clinical and development candidates, including PTK787 (Vatalanib™) and ZD6474 (Vandetanib™). The analogues presented in this *Letter* are potentially useful in the treatment of conditions such as cancer.

Acknowledgments

We thank Dr. J. Doody and Dr. Y. Hadari of *ImClone Systems Inc.* for developing enzymatic and cellular assay conditions published in our earlier studies.[19,20]

References and notes

1. Risau, W. *Nature* **1997**, *386*, 671.
2. Klagsburn, M.; Moses, M. A. *Chem. Biol.* **1999**, *6*, R217.
3. Hanahan, D.; Folkman, J. *Cell* **1996**, *86*, 353.
4. Eskens, F. *Br. J. Cancer* **2004**, *90*, 1.
5. Eskens, F.; Olsson, A.-K.; Dimberg, A.; Kreuger, J.; Claesson-Welsh, L. *Nat. Rev. Mol. Cell Biol.* **2006**, *7*, 359.
6. Zachary, I. *Biochem. Soc. Trans.* **2003**, *31*, 1171.
7. Ferrara, N.; Hillan, K. J.; Gerber, H. P.; Novotny, W. *Nature Rev. Drug Discov.* **2004**, *3*, 391.
8. Saaristo, A.; Karpanen, T.; Alitalo, K. *Oncogene* **2000**, *19*, 6122.
9. Folkman, J. *Nat. Med.* **1995**, *1*, 27.
10. Fuh, G.; Li, B.; Crowley, C.; Cunningham, B. C.; Wells, J. A. *J. Biol. Chem.* **1998**, *273*, 11197.
11. Barleon, B.; Totzke, F.; Herzog, C.; Blanke, S.; Kremmer, E.; Siemeister, G.; Marme, D.; Martiny-Baron, G. *J. Biol. Chem.* **1997**, *272*, 10382.
12. Kiselyov, A. S.; Balakin, K.; Tkachenko, S. E. *Expert. Opin. Invest. Drugs* **2007**, *16*, 83.
13. The anti-angiogenic antibody Avastin™ (Bevacizumab, Genentech, San Francisco, CA) has recently been approved for the treatment of colorectal cancer, see Culy, C. *Drugs Today* **2005**, *41*, 23.
14. The anti-angiogenic aptamer Macugen™ (Pegaptanib sodium, Eyetech Pharmaceuticals, New York, NY and Pfizer) has recently been approved to treat neovascular age-related macular degeneration; see Fine, S. L.; Martin, D. F.; Kirkpatrick, P. *Nat. Rev. Drug Disc.* **2005**, *4*, 187.
15. Ciardello, F.; Caputo, R.; Damiano, V.; Caputo, R.; Troiani, T.; Vitagliano, D.; Carlomagno, F.; Veneziani, B. M.; Fontanini, G.; Bianco, A. R.; Tortora, G. *Clin. Cancer Res.* **2003**, *9*, 1546.
16. Drevs, J.; Konerding, M. A.; Wolloscheck, T.; Wedge, S. R.; Ryan, A. J.; Ogilvie, D. J.; Esser, N. *Angiogenesis* **2004**, *7*, 347.
17. Hess-Stumpp, H.; Haberey, M.; Thierauch, K. H. *Chembiochem* **2005**, *6*, 550.
18. Manley, P. W.; Furet, P.; Bold, G.; Bruggen, J.; Mestan, J.; Meyer, T.; Schnell, C. R.; Wood, J. *J. Med. Chem.* **2002**, *45*, 5687.
19. Piatnitski, E. L.; Duncton, M.; Katoch-Rouse, R.; Sherman, D.; Kiselyov, A. S.; Milligan, D.; Balagtas, C.; Wong, W.; Kawakami, J.; Doody, J. *Bioorg. Med. Chem. Lett.* **2005**, *15*, 4696.
20. Duncton, M.; Piatnitski, E. L.; Kiselyov, A. S.; Milligan, D.; Balagtas, C.; Smith, L., II; Katoch-Rouse, R.; Sherman, D.; Doody, J. *Bioorg. Med. Chem. Lett.* **2006**, *16*, 1579.
21. Kiselyov, A. S.; Semenova, M.; Semenov, V. V.; Piatnitski, E. L. *Chem. Biol.& Drug Design* **2006**, *68*, 250.
22. Kiselyov, A. S.; Semenov, V. V.; Milligan, D. *Chem. Biol.& Drug Design* **2006**, *68*, 308.
23. Kiselyov, A. S.; Piatnitski, L. E.; Samet, A. V.; Kisly, V. P.; Semenov, V. V. *Bioorg. Med. Chem. Lett.* **2007**, *17*, 1369.
24. (a) Gill, M. L.; Frederickson, M.; Cleasby, A.; Woodhead, S. J.; Carr, M. G.; Woodhead, A. J.; Walker, M. T.; Congreve, M. S.; Devine, L. A.; O'Reilly, D.; Seavers, L. C. A.; Davis, D. J.; Curry, J.; Anthony, R.; Padova, A.; Murray, C. W.; Carr, R. A. E.; Jhoti, H. *J. Med. Chem.* **2005**, *48*, 414; (b) Kaiser, K.; Spagnuolo, C. J.; Adams, T. C.; Audia, V. H.; Dupont, A. C.; Hatoum, H.; Lowe, V. C.; Prosser, J. C.; Sturm, B. L.; Noronha, L. *J. Med. Chem.* **1992**, *35*, 4415; (c) Deredas, D.; Frankowski, A. *Carbohydr. Res.* **1994**, *252*, 275.
25. *Analytical data for selected compounds: N*-(4-Chlorophenyl)-1-(2-(pyridin-4-yl)ethyl)-1*H*-pyrazole-5-carboxamide (**11**), mp 193–195 °C; ^{1}H NMR (400 MHz, dmso-d_6; δ, ppm): 2.98 (t, J = 9.2 Hz, 2H), 4.11 (t, J = 9.2 Hz, 2H), 6.88 (d, J = 6.4 Hz, 1H), 7.25 (d, J = 7.2 Hz, 2H), 7.38 (d, J = 8.4 Hz, 2H), 7.69 (d, J = 6.4 Hz, 1H), 7.76 (d, J = 8.4 Hz, 2H), 8.65 (d, J = 7.2 Hz, 2H), 12.5 (br s, D_2O, 1 H, *N*HCO); ^{13}C NMR (100 MHz, dmso-d_6; δ, ppm): 33.8, 56.5, 107.3, 122.5, 122.9, 128.5, 129.6, 131.3, 134.6, 140.2, 148.4, 150.1, 163.0; ESI MS (M+1): 328, (M-1): 326; HRMS, exact mass calcd. for $C_{17}H_{15}ClN_4O$: 326.0934, found: 326.0932. Elemental analysis: calcd for $C_{17}H_{15}ClN_4O$: C, 62.48; H, 4.63; N, 17.15; found: C, 62.21; H, 4.77, N, 16.93.
1-(2-(Pyridin-4-yl)ethyl)-*N*-(4-(trifluoromethyl)phenyl)-1*H*-pyrazole-5-carboxamide (**18**), mp 227–229 °C; ^{1}H NMR (400 MHz, dmso-d_6; δ, ppm): 3.04 (t, J = 9.2 Hz, 2H), 4.05 (t, J = 9.2 Hz, 2H), 6.74 (d, J = 6.4 Hz, 1H), 7.29 (d, J = 7.2 Hz, 2H), 7.39 (d, J = 8.4 Hz, 2H), 7.65 (d, J = 6.4 Hz, 1H), 7.78 (d, J = 8.4 Hz, 2H), 8.71 (d, J = 7.2 Hz, 2H), 13.1 (br s, D_2O, 1 H, *N*HCO); ^{13}C NMR (100 MHz, dmso-d_6; δ, ppm): 33.8, 57.5, 107.9, 121.7, 122.3, 122.8, 123.5, 125.9, 126.3, 134.9, 140.6, 148.5, 150.3, 162.9; ESI MS (M+1): 361, (M-1): 359; HRMS, exact mass calcd. for $C_{18}H_{15}F_3N_4O$: 360.1198, found: 360.1195. Elemental analysis: calcd for $C_{18}H_{15}F_3N_4O$: C, 60.00; H, 4.20; N, 15.55; found: C, 59.74; H, 4.03, N, 15.36.
N-(4-(Chlorodifluoromethoxy)phenyl)-1-(2-(pyridin-4-yl)ethyl)-1*H*-pyrazole-5-carboxamide(**22**), mp 241–223 °C; ^{1}H NMR (400 MHz, dmso-d_6; δ, ppm): 3.04 (t, J = 9.2 Hz, 2H), 4.05 (t, J = 9.2 Hz, 2H), 6.74 (d, J = 6.4 Hz, 1H), 7.29 (d, J = 7.2 Hz, 2H), 7.39 (d, J = 8.4 Hz, 2H), 7.65 (d,

J = 6.4 Hz, 1H), 7.78 (d, J = 8.4 Hz, 2H), 8.71 (d, J = 7.2 Hz, 2H), 13.1 (br s, D_2O, 1H, *N*HCO); ^{13}H NMR (100 MHz, dmso-d_6; δ, ppm): 33.9, 58.2, 107.8, 115.3, 122.5, 122.9, 128.0, 129.8, 140.1, 148.3, 150.5, 155.6, 162.9, 166.6; ESI MS (M+1): 394,(M−1): 392; HRMS, exact mass calcd. for $C_{18}H_{15}ClF_2N_4O_2$: 392.0852, found: 392.0850. Elemental analysis: calcd for $C_{18}H_{15}ClF_2N_4O_2$: C, 55.04; H, 3.85; N, 14.26; found: C, 54.83; H, 3.67, N, 14.05.

N-(4-*tert*-Butylphenyl)-1-(2-(pyridin-4-yl)ethyl)-1*H*-pyrazole-5-carboxamide (**23**), mp 207–209 °C; 1H NMR (400 MHz, dmso-d_6; δ, ppm): 1.29 (s, 9H, *t*Bu), 3.02 (t, J = 9.2 Hz, 2H), 4.07 (t, J = 9.2 Hz, 2H), 6.79 (d, J = 6.4 Hz, 1H), 7.27 (d, J = 7.2 Hz, 2H), 7.34 (d, J = 8.4 Hz, 2H), 7.66 (d, J = 6.4 Hz, 1H), 7.71 (d, J = 8.4 Hz, 2H), 8.67 (d, J = 7.2 Hz, 2H), 12.9 (br s, D_2O, 1 H, *N*HCO); ^{13}C NMR (100 MHz, dmso-d_6; δ, ppm): 29.8, 33.9, 41.2, 56.7, 107.6, 121.9, 122.7, 128.4, 129.3, 131.1, 134.9, 140.6, 148.9, 150.3, 163.4; ESI MS (M+1): 349, (M-1): 347; HRMS, exact mass calcd. for $C_{21}H_{24}N_4O$: 348.1950, found: 348.1947. Elemental analysis: calcd for $C_{21}H_{24}N_4O$: C, 72.39; H, 6.94; N, 16.08; found: C, 72.17; H, 6.79, N, 15.87.

N-(4-Chlorophenyl)-3-methyl-1-(2-(pyridin-4-yl)ethyl)-1*H*-pyrazole-5-carboxamide (**35**), mp 198–199 °C; ^{1}H NMR (400 MHz, dmso-d_6; δ, ppm): 2.88 (s, 3H, CH_3), 3.01 (t, J = 9.2 Hz, 2H), 4.02 (t, J = 9.2 Hz, 2 H), 6.53 (s, 1H), 7.22 (d, J = 7.2 Hz, 2H), 7.34 (d, J = 8.4 Hz, 2H), 7.67 (d, J = 8.4 Hz, 2H), 8.66 (d, J = 7.2 Hz, 2H), 12.3 (br s, D_2O, 1H, *N*HCO); ^{13}C NMR (100 MHz, dmso-d_6; δ, ppm): 18.0, 33.7, 58.0, 104.2, 122.6, 123.1, 128.8, 129.7, 134.5, 140.1, 146.3, 148.5, 150.3, 162.4; ESI MS (M+1): 342, (M−1): 340; HRMS, exact mass calcd. for $C_{18}H_{17}ClN_4O$: 340.1091, found: 340.1089. Elemental analysis: calcd for $C_{18}H_{17}ClN_4O$: C, 63.44; H, 5.03; N, 16.44; found: C, 63.26; H, 4.87, N, 16.27.

N-(4-Chlorophenyl)-3,4-dimethyl-1-(2-(pyridin-4-yl)ethyl)-1*H*-pyrazole-5-carboxamide (**37**), mp 211–213 °C; ^{1}H NMR (400 MHz, dmso-d_6; δ, ppm): 2.06 (s, 3H, CH_3), 2.75 (s, 3H, CH_3), 3.00 (t, J = 9.2 Hz, 2H), 4.01 (t, J = 9.2 Hz, 2H), 7.29 (d, J = 7.2 Hz, 2H), 7.39 (d, J = 8.4 Hz, 2H), 7.68 (d, J = 8.4 Hz, 2H), 8.65 (d, J = 7.2 Hz, 2H), 12.3 (br s, D_2O, 1H, *N*HCO); ^{13}C NMR (100 MHz, dmso-d_6; δ, ppm): 10.5, 13.2, 33.9, 58.5, 115.2, 122.7, 123.0, 128.9, 130.5, 133.4, 144.7, 145.5, 150.1, 162.4; ESI MS (M+1): 356, (M−1): 354; HRMS, exact mass calcd. for $C_{19}H_{19}ClN_4O$: 354.1247, found: 354.1244. Elemental analysis: calcd for $C_{19}H_{19}ClN_4O$: C, 64.31; H, 5.40; N, 15.79; found: C, 64.12; H, 5.27, N, 15.63.

N-(4-Chlorophenyl)-1-(2-(pyridin-4-yl)ethyl)-1*H*-indole-2-carboxamide (**39**), mp 227–228 °C; ^{1}H NMR (400 MHz, dmso-d_6; δ, ppm): 3.05 (t, J = 9.2 Hz, 2H), 4.11 (t, J = 9.2 Hz, 2H), 7.05 (m, 1H), 7.14 (d, J = 8.4, 1H), 7.26 (d, J = 7.2 Hz, 2H), 7.34 (d, J = 8.4 Hz, 2H), 7.37 (s, 1H), 7.41 (m, 1H), 7.55 (d, J = 8.0 Hz, 1H), 7.65 (d, J = 8.4 Hz, 2H), 8.62 (d, J = 7.2 Hz, 2H), 12.1 (br s, D_2O, 1H, *N*HCO); ^{13}C NMR (100 MHz, dmso-d_6; δ, ppm): 36.7, 58.3, 109.8, 115.0, 117.7, 119.8, 120.5, 122.3, 123.1, 123.4, 128.8, 129.8, 131.3, 134.0, 141.7, 148.5, 150.4, 162.4; ESI MS (M+1): 377, (M-1): 375; HRMS, exact mass calcd for $C_{22}H_{18}ClN_3O$: 375.1138, found: 375.1136. Elemental analysis: calcd for $C_{22}H_{18}ClN_3O$: C, 70.30; H, 4.83; N, 11.18; found: C, 70.05; H, 4.66, N, 10.97.

N-(4-Chlorophenyl)-1-(2-(pyridin-4-yl)ethyl)-1*H*-imidazole-2-carboxamide (**41**), mp 175–176 °C; ^{1}H NMR (400 MHz, dmso-d_6; δ, ppm): 3.02 (t, J = 9.2 Hz, 2H), 4.11 (t, J = 9.2 Hz, 2H), 7.28 (d, J = 6.0 Hz, 1H), 7.31 (d, J = 7.2 Hz, 2H), 7.39 (d, J = 8.4 Hz, 2H), 7.56 (d, J = 6.0 Hz, 1H), 7.68 (d, J = 8.4 Hz, 2H), 8.75 (d, J = 7.2 Hz, 2H), 12.5 (br s, 1H, NH); ^{13}C NMR (100 MHz, dmso-d_6; δ, ppm): 35.3, 54.0, 121.9, 123.4, 128.7, 128.9, 129.9, 131.3, 133.4, 148.5, 149.8, 153.6, 158.2; ESI MS (M+1): 328, (M−1): 326; HRMS, exact mass calcd for $C_{17}H_{15}ClN_4O$: 326.0934, found: 326.0931. Elemental analysis: calcd for $C_{17}H_{15}ClN_4O$: C, 62.48; H, 4.63; N, 17.15; found: C, 62.27; H, 4.48, N, 16.93.

N-(4-Chlorophenyl)-1-(2-(pyridin-4-yl)ethyl)-1*H*-benzo[d]-imidazole-2-carboxamide (**46**), mp 245–248 °C; ^{1}H NMR (400 MHz, dmso-d_6; δ, ppm): 3.07 (t, J = 9.2 Hz, 2H), 4.15 (t, J = 9.2 Hz, 2H), 7.15 (m, 1H), 7.24 (m, 1H), 7.29 (d, J = 7.2 Hz, 2H), 7.38(d, J = 8.4 Hz, 2H), 7.58 (d, J = 8.0Hz, 1H), 7.65 (d, J = 8.4 Hz, 2H), 7.81 (d, J = 8.0 Hz, 1H), 8.66 (d, J = 7.2 Hz, 2H), 12.8 (br s, D_2O, 1H, *N*HCO); ^{13}C NMR (100 MHz, dmso-d_6; δ, ppm): 36.9, 55.1, 113.9, 115.3, 117.9, 122.7, 123.1, 123.6, 129.2, 129.5, 133.6, 134.0, 139.2, 141.6, 148.9, 150.3, 156.9; ESI MS (M+1): 378, (M−1): 376; HRMS, exact mass calcd. for $C_{21}H_{17}ClN_4O$: 376.1091, found: 376.1088. Elemental analysis: calcd for $C_{21}H_{17}ClN_4O$: C, 66.93; H, 4.55; N, 14.87; found: C, 66.75; H, 4.36, N, 14.64.

N-(4-Chlorophenyl)-1-(2-(pyridin-4-yl)ethyl)-1*H*-tetrazole-5-carboxamide (**49**), mp 169–171 °C; ^{1}H NMR (400 MHz, dmso-d_6; δ, ppm): 3.09 (t, J = 9.2 Hz, 2H), 4.17 (t, J = 9.2 Hz, 2H), 7.33 (d, J = 7.2 Hz, 2H), 7.41 (d, J = 8.4 Hz, 2H), 7.69 (d, J = 8.4 Hz, 2H), 8.78 (d, J = 7.2 Hz, 2H), 12.7 (br s, 1H, NH); ^{13}C NMR (100 MHz, dmso-d_6; δ, ppm): 36.2, 53.7, 122.6, 123.5, 129.0, 129.9, 134.3, 148.9, 150.5, 155.1, 158.3; ESI MS (M+1): 330, (M−1): 328; HRMS, exact mass calcd for $C_{15}H_{13}ClN_6O$: 328.0839, found: 328.0836. Elemental analysis: calcd for $C_{15}H_{13}ClN_6O$: C, 54.80; H, 3.99; N, 25.56; found: C, 54.61; H, 3.81, N, 25.33.

N-(4-Chlorophenyl)-*N*-methyl-1-(2-(pyridin-4-yl)ethyl)-1*H*-pyrazole-5-carboxamide (**54**), mp 181–182 °C; ^{1}H NMR (400 MHz, dmso-d_6; δ, ppm): 2.66 (s, 3H, CH_3), 3.01 (t, J = 9.2 Hz, 2H), 4.09 (t, J = 9.2 Hz, 2H), 6.82 (d, J = 6.4 Hz, 1H), 7.31 (d, J = 7.2 Hz, 2H), 7.33 (d, J = 8.4 Hz, 2H), 7.55 (d, J = 6.4 Hz, 1H), 7.78 (d, J = 8.4 Hz, 2H), 8.61 (d, J = 7.2 Hz, 2H); ^{13}C NMR (100 MHz, dmso-d_6; δ, ppm): 29.7, 33.3, 57.1, 107.9, 122.4, 122.7, 128.6, 129.5, 131.9, 135.1, 140.4, 149.0, 150.6, 159.7; ESI MS (M+1): 342, (M-1): 340; HRMS, exact mass calcd. for $C_{18}H_{17}ClN_4O$: 340.1091, found: 340.1087. Elemental analysis: calcd for $C_{18}H_{17}ClN_4O$: C, 63.44; H, 5.03; N, 16.44; found: C, 63.27; H, 4.91, N, 16.28.

26. VEGFR-2 kinase inhibition was determined by measuring the phosphorylation level of *poly*-Glu-Ala-Tyr-biotin (*p*GAT-biotin) peptide in HTRF assay.Into a 96-well Costar plate was added 2 μl/well of 25× compound in a 100% DMSO (final concentration in the 50 μl kinase reaction was typically 1 nM to 10 μM). Next, 38 μl of reaction buffer (25 mM Hepes, pH 7.5, 5 mM $MgCl_2$, 5 mM $MnCl_2$, and 2 mM DTT, 1 mg/ml BSA) containing 0.5 mmol pGAT-biotin and 3–4 ng KDR enzyme was added to each well. After 5–10-min preincubation, the kinase reaction was initiated by the addition of 10 μl of 10 μM ATP in the reaction buffer, after which the plate was incubated at room temperature for 45 min. The reaction was stopped by addition of 50 μl of KF buffer (50 mM Hepes, pH 7.5, 0.5 M KF, and 1 mg/ml BSA) containing 100 mM EDTA and 0.36 μg/ml PY20K (Eu-cryptate labeled anti-phosphotyrosine antibody, CIS bio international) was added and after an additional 2 h incubation at RT, the plate was analyzed in a RUBYstar HTRF Reader.
27. Cytotoxicity of this molecule was further after treatment of A431, DLD1, and DU145 cells for 24 h with **34**; GI_{50} values for these cell lines were 50, 125, and 220 nM, respectively. GI_{50} represents the concentration of compound that caused 50% reduction in absorbance at 562 nm relative to untreated cells using sulfurhodamine B assay. Values were means of three independent determinations (SD < 10%).

28. McTigue, M. A.; Wickersham, J. A.; Pinko, C.; Showalter, R. E.; Parast, C. V.; Tempczyk-Russell, A.; Gehring, M. R.; Mroczkowski, B.; Kan, C. C.; Villafranca, J. E.; Appelt, K. *Structure* **1999**, *7*, 319.
29. Berman, H. M.; Westbrook, J.; Feng, Z.; Gilliland, G.; Bhat, T. N.; Weissig, H.; Shindyalov, I. N.; Bourne, P. E. *The Protein Data Bank Nucl. Acids Res.* **2000**, *28*, 235.
30. Jain, R. K. *Science* **2005**, *307*, 58.
31. Cell-based assay for VEGFR-2 inhibition: (i) *Transfection of 293 cells with DNA expressing FGFR1/VEGFR-2 chimera*: A chimeric construct containing the extracellular portion of FGFR1 and the intracellular portion of VEGFR-2 was transiently transfected into 293 adenovirus-transfected kidney cells. DNA for transfection was diluted to a 5 μg/ml final concentration in a serum-free medium and incubated at room temperature for 30 min with 40 μl/ml of Lipofectamine 2000, also in serum-free media. 25 μl of the Lipofectamine/DNA mixture was added to 293 cells suspended at 5×10^5 cells/ml. 200 μl/well of the suspension was added to a 96-well plate and incubated overnight. Within 24 h, media were removed and 100 μl of media with 10% fetal bovine serum was added to the now adherent cells followed by an additional 24-h incubation. Test compounds were added to the individual wells (final DMSO concentration was 0.1%). Cells were lysed by re-suspension in 100 μl Lysis buffer (150 mM NaCl, 50 mM Hepes, pH 7.5, 0.5% Triton X-100, 10 mM NaPPi, 50 mM NaF, and 1 mM Na_3VO_4) and rocked for 1 h at 4 °C; (ii) *ELISA for detection of tyrosine-phosphorylated chimeric receptor*: 96-well ELISA plates were coated using 100 μl/well of 10 μg/ml of αFGFR1 antibody and incubated overnight at 4 °C. αFGFR1 was prepared in a buffer made with 16 ml of a 0.2 M Na_2CO_3 and 34 ml of a 0.2 M $NaHCO_3$ with pH adjusted to 9.6. Concurrent with lysis of the transfected cells, αFGFR1 coated ELISA plates were washed three times with PBS + 0.1% Tween 20, blocked by addition of 200 μl/well of a 3% BSA in PBS for 1 h, and washed again. 80 μl of lysate was then transferred to the coated and blocked wells and incubated for 1 h at 4 °C. The plates were washed three times with PBS + 0.1% Tween 20. To detect bound phosphorylated chimeric receptor, 100 μl/well of anti-phosphotyrosine antibodies (RC20:HRP), Transduction Laboratories)) was added (final concentration 0.5 μg/ml in PBS) and incubated for 1 h. The plates were washed six times with PBS + 0.1% Tween 20. Enzymatic activity of HRP was detected by adding 50 μl/well of equal amounts of the Kirkegaard & Perry Laboratories (KPL) Substrate A and Substrate B. The reaction was stopped by addition of 50 μl/well of a 0.1 N H_2SO_4, absorbance was measured at 450 nm.